Biosensors and Bioelectronics 47 (2013) 271–277

Contents lists available at SciVerse ScienceDirect

Biosensors and Bioelectronics

journal homepage: www.elsevier.com/locate/bios

Electrochemiluminescence of blue-luminescent graphene quantum dots and its application in ultrasensitive aptasensor for adenosine triphosphate detection

Juanjuan Lu [a], Mei Yan [a], Lei Ge [a], Shenguang Ge [b], Shaowei Wang [a], Jixian Yan [a], Jinghua Yu [a,*]

[a] Key Laboratory of Chemical Sensing & Analysis in Universities of Shandong, School of Chemistry and Chemical Engineering, University of Jinan, Jinan 250022, PR China

[b] Shandong Provincial Key Laboratory of Preparation and Measurement of Building Materials, University of Jinan, Jinan 250022, PR China

ARTICLE INFO

Article history:
Received 23 February 2013
Received in revised form
18 March 2013
Accepted 18 March 2013
Available online 27 March 2013

Keywords:
Graphene quantum dots
Electrochemiluminescence
SiO_2 nanospheres
Aptamer
ATP

ABSTRACT

A simple approach based on exfoliating and disintegrating treatments for graphite oxide, followed by hydrothermal synthesis, was developed to prepare water-soluble graphene quantum dots (GQDs). The as-prepared GQDs exhibited bright blue emission under ultraviolet irradiation (~365 nm), and showed an excitation-independent photoluminescence feature. More importantly, a newly anodic electrochemiluminescence (ECL) was observed from the water-soluble GQDs with H_2O_2 as coreactant for the first time, and the ECL induced a strong light emission at a low potential (ca. 0.4 V vs. Ag/AgCl). The ECL mechanism is investigated in detail. Employing SiO_2 nanospheres as signal carrier, a novel SiO_2/GQDs ECL signal amplification labels were synthesized based on which a ultrasensitive ECL aptamer sensor was proposed. Under the optimized experimental conditions, the proposed ECL aptamer sensor exhibited excellent analytical performance for adenosine triphosphate (ATP) determination, ranging from 5.0×10^{-12} to 5.0×10^{-9} mol L^{-1} with the detection limit of 1.5×10^{-12} mol L^{-1}. Due to the low cytotoxicity and excellent biocompatibility, GQDs are demonstrated to be an eco-friendly material as well as excellent ECL labeling agents for biosensor.

1. Introduction

Highly luminescent semiconductor nanocrystals (NCs), often referred to as quantum dots (QDs), have generated much excitement for a wide variety of promising applications in optoelectronic devices, biological labeling and biomedicine. Some NCs, such as CdS (Myung et al., 2002), CdTe (Bae et al., 2004) and CdSe/ZnSe (Myung et al., 2003), can be used as electrochemiluminescence (ECL) regents in bioanalytical applications (Shan et al., 2010; Jie et al., 2009; Zou et al., 2011). Although these semiconductor QDs have been accepted as ECL indicators for their effective and valuable ECL behavior, one challenge regarding these heavy metals have raised serious health and environmental concerns (Derfus et al., 2004). Therefore, searching for benign nanomaterials with good ECL activities has become an urgent challenge.

Graphene, a single layer of carbon atoms densely packed in honeycomb two-dimensional (2D) lattice, has extensive applications in physics, chemistry and material science, owing to its unique electronic, thermal, mechanical and chemical properties (Rümmeli et al., 2011; Yang et al., 2010). However, graphene s a zero-bandgap semiconductor, which limits its electronic and optoelectronic application. Due to the lack of a bandgap, no optical luminescence is observed in pristine graphene (Eda et al., 2010; Loh et al., 2010). It has been both theoretically predicted and experimentally proven that the properties of graphene sheets can effectively determined by their morphology, including size, shape and thickness (Kosynkin et al., 2009). To effectively tune the bandgap of graphene, promising approach is to convert the 2D graphene sheets into 0D graphene quantum dots (GQDs). GQDs, as recently emerging carbon-based materials, are graphene sheets smaller than 100 nm (Ponomarenko et al., 2008). They exhibit new phenomena due to quantum confinement and edge effects. GQDs are attracting considerable attention as they may gradually replace traditional semiconductor QDs due to their superiority in chemical inertness, low toxicity biocompatibility, high fluorescent activity and excellent photostability (Zhu et al., 2011; Zong et al., 2011). However, the development and application of GQDs remain inchoate, and the synthesis is only a recent effort.

In this work, we report a simple method to obtain water-soluble GQDs based on exfoliating and disintegrating of graphite oxide, followed by hydrothermal process. The as-prepared

* Corresponding author. Tel.: +86 531 82767161; fax: +86 531 82971177.
E-mail addresses: ujn.yujh@gmail.com, 306375767@qq.com (J. Yu).

0956-5663/$ - see front matter © 2013 Elsevier B.V. All rights reserved.
http://dx.doi.org/10.1016/j.bios.2013.03.039

products exhibited bright blue emission under ultraviolet irradiation (~365 nm) in a water solution of neutral pH, and showed an excitation-independent photoluminescence feature. Most interestingly, they also exhibited a novel anodic ECL by using H_2O_2 as coreactant, and the mechanism was investigated in detail. Compared with reported cathodic ECL of GQDs using $K_2S_2O_8$ as coreactant (Li et al., 2012), the as-prepared GQDs showed an anodic ECL at a relatively lower potential (ca. 0.4 V vs. Ag/AgCl). Such low potential can avoid the damage of the modified electrodes and biomolecules, supplying a high stability of the ECL biosensor for biomarker detection.

Adenosine triphosphate (ATP) is generally acknowledged as "energy currency " in most animate beings, and plays an important role in most enzymatic activities (Yan et al., 2010a). The concentration and dissipative rate of ATP have been found to be closely related to many diseases such as hypoxia, hypoglycemia, ischemia, Parkinson's disease and some malignant tumors. The detection of ATP is not only of research interest but of clinical importance. Various methods such as fluorescence and colorimetric approaches have been developed to detect ATP (Robert et al., 2002; Jose et al., 2007). In recent years, with the increasing applications of aptamer as a new recognition element, some novel aptamer-based approaches for ATP determination have been developed. Aptamers are nucleic acid macromolecules of single-stranded DNA/RNA oligonucleotides which can bind with a wide array of targets with high affinity and specificity (Tuerk and Gold, 1990; Ellington and Szostak, 1990). Due to their easy labeling, high stability and specificity, particular attention has been paid to the development of aptamer-based sensors (Willner and Zayats, 2007; Famulok et al., 2007; Zuo et al., 2007; Xiao et al., 2005). ECL is a kind of chemiluminescent reaction triggered by electrochemical methods. In comparison to other sensors based on fluorescence or other spectroscopic methods, most sensor based on ECL detection own the remarkable features of high sensitivity and low detection limits (Hu and Xu, 2010; Miao, 2008). The combination of high sensitivity of the ECL technique and high selectivity of aptamer has led the emergence of ECL aptamer sensor (Fang et al., 2008; Li et al., 2008).

Herein, a ultrasensitive ECL aptamer sensor for ATP was proposed based on intense ECL of GQDs. The most effective strategy for signal amplification in ECL biosensor can be simply realized by employing a carrier loaded with large amounts of labels instead of traditional single-type label. It has been reported that SiO_2 nanospheres are well recognized as commonly used nanocarriers because of their excellent water-solubility, simple surface functionalization, and good biocompatibility (Wu et al., 2009; Chen et al., 2009; Qian et al., 2010; Yuan et al., 2011). Hence, a novel ECL signal amplifier, GQDs doped SiO_2 nanospheres (SiO_2/GQDs) was applied to modify the aptamer DNA. Such ECL aptamer sensor based on SiO_2/GQDs exhibited excellent analytical performance for ATP determination. Owing to their chemical inertness, low cytotoxicity and attractive biocompatibility, GQDs are demonstrated to be an eco-friendly material as well as excellent ECL labeling agents for biosensor.

2. Experimental

2.1. Chemicals

Chemicals and materials: Graphite powder (KS-10, 99.95%), N-hydroxysuccinimide (NHS), N-(3-dimethylamminopropyl)-N′-ethylcarbodiimide hydrochloride (EDC), 6-mercapto-1-hexanol (MCH) were obtained from Sigma-Aldrich. (3-aminopro-pyl)-triethoxy-silane (APTES) was purchased from Alfa Aesar China Ltd. ATP, cytidine triphosphate (CTP), guanosine triphosphate (GTP), uridine triphosphate (UTP) were purchased from Aladdin Chemistry Co., Ltd. Phosphate buffered solutions (PBS) were prepared using 0.01 mol L^{-1} KH_2PO_4 and 0.01 mol mol L^{-1} Na_2HPO_4. All other reagents were of analytical reagent grade and used without further purification. Ultrapure water obtained from a Millipore water purification system (≥18 MΩ, Milli-Q, Millipore) was used in all assays and solutions.

All oligonucleotides used in this study were purchased from Sangon Biotech Co., Ltd. (Shanghai, China), and the sequences of oligonucleotides were as follows:

- ssDNA1: 5′-HS-$(CH_2)_6$-ACCTGGGGGAGTAT-3′;
- ssDNA2: 5′-TGCGGAGGAAGGT-NH_2-3′.

2.2. Apparatus

The ECL experiments were carried out on a MPI-B multiple-parameter chemiluminescence analytical testing system equipped with a MPI-A/B multifunction chemiluminescence detector (Xi′An Remax Electronic Science & Technology Co. Ltd. Xi′an, Changchun Institute of Applied Chemistry Chinese Academy Sciences, China) at room temperature. Cyclic voltammetric (CV) measurements were performed with a CHI 760D electrochemical workstation (Shanghai CH Instruments, China). All experiments were carried out with a conventional three-electrode system with Au as the working electrode (WE), a platinum counter electrode (CE) and an Ag/AgCl (sat. KCl) reference electrode (RE). Au working electrodes were cleaned by using the electrochemical technique in 0.1 M H_2SO_4 with a high scan rate of 0.5 V s^{-1} and potential scanning between −0.2 and 1.4 V until a reproducible CV was obtained. UV–vis spectra were recorded on a UV-3600 spectrophotometer (Shimadzu, Kyoto, Japan). Photoluminescence spectra were obtained on a RF-5301PC spectrophotometer (Shimadzu, Kyoto, Japan).Scanning electron microscopy (SEM) images were recorded using a JEOL-JSM-6300 scanning electron microscope. Transmission electron microscopy (TEM) images were obtained from a Hitachi H-800 microscope (Japan). High resolution transmission electron microscopy (HRTEM) image of the prepared C-dots were recorded on an electronic microscopy (Tecnai G2 F20S5TWIN 200 KV). Atomic force microscope (AFM) images were achieved by scanning probe microscopy (SPM, Vecco, USA).

2.3. Synthesis of GQDs

Graphene oxide (GO) was synthesized from natural graphite powder by an improved Hummers method (Marcano et al., 2010). GO was dissolved in water with the concentration of 100 mg mL^{-1}. The suspension was disrupted into a homogeneous solution using an ultrasonic cell crusher for 60 min. Ultrasound can generate alternating low-pressure and high-pressure waves in liquid, leading to the formation and violent collapse of small vacuum bubbles. These cavitations cause high-speed impinging liquid jets, deagglomeration, and strong hydrodynamic shear forces (Li et al., 2011). Then, the homogeneous solution was transferred into a poly (tetrafluoroethylene) (Teflon)-lined autoclave (30 mL) and heated at 200 °C for 10 h. The as-prepared products contained brown transparent suspension and black precipitates, and the black precipitates were wasted. The resulting solution was further dialyzed in a dialysis bag (retained molecular weight: 3500 Da) to obtain GQDs, and the GQDs have excellent solubility in many polar organic solvents or water with different pH levels. The final obtained solution was fully stable for more than three months when kept in refrigerator at 4°C.

2.4. Synthesis of SiO_2/GQDs

Monodispersed SiO_2 nanospheres, used as carriers for GQDs and ssDNA2 immobilization, were synthesized according to previously reported method (Joo et al., 2012) with slight modification. The procedure was briefly described as follows. Initially, water (4.0 mL), ethanol (10.0 mL) and NH_3•H_2O (2.0 mL) were loaded into the semibatch reactor. Then, 100 μL of tetraethoxysilane solution was quickly introduced into the system. In order to make it well-distributed, the mixture was under vigorously mechanical stir until equilibrium reached at room temperature. Finally, the precipitated spherical silica particles were separated by centrifugation and washed with ethanol for several times to remove impurities. Dry SiO_2 nanospheres were obtained by drying the residue at 80 °C in vacuum.

For the preparation of SiO_2/GQDs composites, 0.1 g of the prepared SiO_2 nanospheres were first dispersed in 8 mL of ethanol and treated with 1 mL of APTES. After stirring for 6 h, the suspension was centrifuged and washed with ethanol repeatedly for four times and the amino-functionalized SiO_2 nanospheres were obtained. Then, the amino-functionalized SiO_2 nanospheres were dispersed in a mixture of 1.0 mL of the prepared GQDs and 1.0 mL of EDC (10 mg mL^{-1}). The mixed suspension was stirred at 4 °C for 12 h. Unbound GQDs were removed by successive centrifugation and the suspension was washed with water for several times. Finally, the obtained SiO_2/GQDs composites were dispersed in water with a final volume of 1.0 mL for further use.

2.5. Synthesis of SiO_2/GQDs/ssDNA2

0.5 mL of the as-prepared SiO_2/GQDs suspension was mixed with ssDNA2 (1 mL, 50 μM) solution. Subsequently, 200 μL of freshly prepared EDC (20 mg mL^{-1}) and 200 μL of NHS (10 mg mL^{-1}) were added and then incubated for 2 h to form the SiO_2/GQDs/ssDNA2 bioconjugates. The resulting were washed with PBS (pH 7.4) and then redispersed in PBS (pH 7.4, 1 mL) and stored at 4 °C for use.

2.6. Preparation of ECL aptamer sensor

The fabrication of this ECL aptamer sensor based on GQDs ECL is represented in Fig. 1. The detailed fabrication process was as follows: First, 15 μL of 2 μM ssDNA1 solution was dropped onto the pre-cleaned Au electrode. Subsequently, physically absorbed excess ssDNA1s were rinsed with PBS. The ssDNA1 modified electrode was further treated with 1.0 mmol L^{-1} MCH for 1 h to obtain a well-aligned DNA monolayer, followed by washing with the washing buffer and ultrapure water alternately to remove nonspecific adsorption. Eventually, the electrode was immersed into the solution which contains SiO_2/GQDs/ssDNA2 and various concentrations of ATP at room temperature and held for 2 h. After these procedures, the electrode was washed with PBS to remove the excrescent matter.

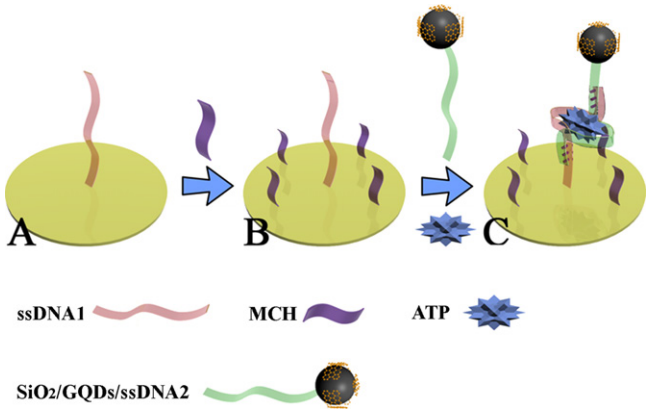

Fig. 1. Schematic representation of the ECL aptamer ATP sensor. (A) Immobilization of ssDNA1 on the surfaces of Au electrode. (B) Treated with MCH to obtain a well-aligned DNA monolayer. (C) Hybridization of the two fragments in the presence of ATP.

3. Results and discussion

3.1. Structural characterization

The graphene oxide was characterized by TEM and AFM. The TEM image (Fig. S1A in supporting information) displays a view of graphene oxide nanosheets clearly illustrating typical flake-like wrinkled shapes of graphene oxide with irregular size. Fig. S1B is the typical AFM images and height profiles of graphene oxide. The thickness of the graphene sheet obtained is about 1 nm, which are consistent with previously reported thickness of single-layer graphene oxide sheets (Marcano et al., 2010).

Fig. 2A and B show the TEM image of GQDs and their size distributions. The diameters were mainly distributed in the range of 4–9 nm with average diameters of 7 nm (Fig. 2C). Inset in Fig. 3B is the representative image of individual GQDs, indicating the high crystallinity of the GQDs.

Proved by Fourier transform infrared (FTIR) spectra, the as-prepared GQDs contain many chemical groups such as –OH, epoxy/ether, C=O, so they posses excellent solubility in water and most polar organic solvents without further chemical modifications, these dispersions are stable at room temperature for at least six months. In the FTIR analysis of GQDs (Fig. 2D), a broad band centered at 3416 cm^{-1} represents free O–H bonding, and C=O were observed at 1383 cm^{-1}. The aromatic ring stretch C=C is revealed due to the band at 1383 cm^{-1}, indicating the delocalization of π-electron. However, the C-O-C stretching vibration peak at 1260 cm^{-1} disappeared entirely in GQDs, which is consistent with previous reports that epoxy groups could serve as chemically reactive sites for the rupture of the underlying C–C bonds (Li et al., 2011).

The morphologies of SiO_2 nanospheres and SiO_2/GQDs were studied by SEM and TEM. Fig. 3A and C indicated that the prepared SiO_2 nanospheres display a resulting clean and structure homogenized microsphere. Coating of the GQDs onto the surface of SiO_2 nanospheres was achieved through acylamide binding in the presence of EDC as the activator. As shown in Fig. 3B and C, GQDs were coating on the surface of SiO_2 uniformly.

3.2. Optical characterization

From the UV–vis absorption of GQDs (Fig. 4A), a typical absorption peak at 305 nm was observed, and the strong background absorption below 250 nm was assigned to the π–π^* transition of aromatic sp^2 domains (Pan et al., 2010). The GQDs aqueous solution exhibited bright blue emission under excitation of 365 nm UV light. To further explore the optical properties of as-synthesized GQDs, a detailed photoluminescence study was carried out by using different excitation wavelengths. Generally speaking, the photoluminescence spectra of most luminescent carbon nanoparticles are dependent on excitation wavelength. In other words, the photoluminescence peaks shifted to longer wavelengths with a maximum intensity as the excitation wavelength was a bathochromic shift. However, the as-prepared GQDs in this work showed an excitation-independent photoluminescence feature. When the excitation wavelength changes from 260 to 380 nm, the photoluminescence spectra are almost invariable and show a strong peak at ca.450 nm (Fig. 4B). In order to confirm

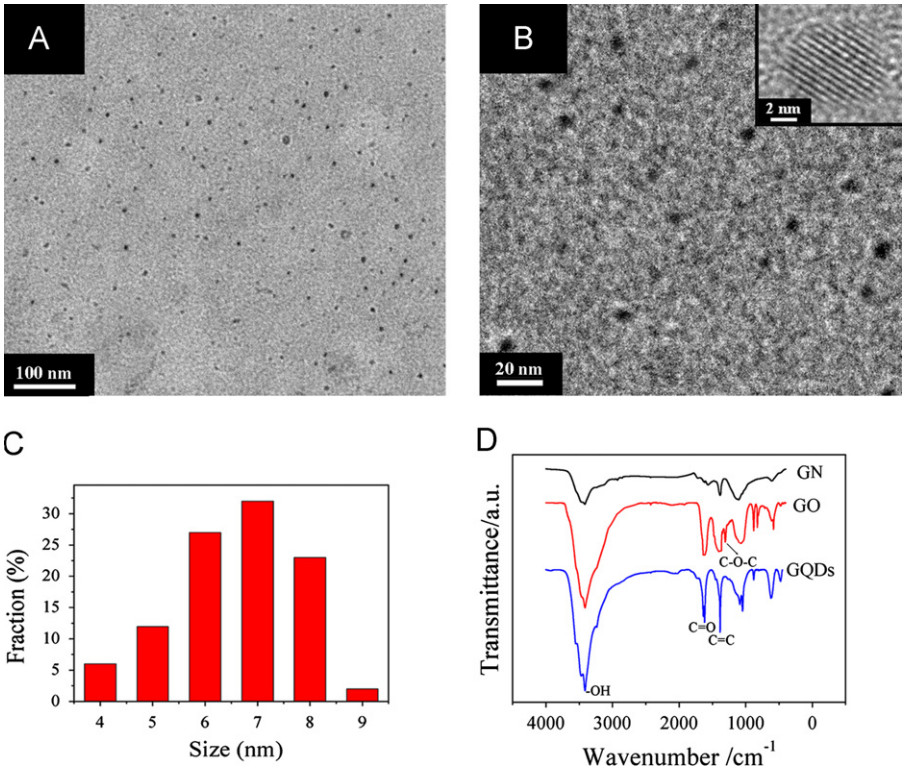

Fig. 2. Structural characterization of GQDs. TEM image of the GQDs (A), (B) and their size distributions (C), inset of (B) shows HRTEM of individual GQDs, (D) FTIR spectra of GN (graphene), GO and GQDs.

that GQDs have been anchored onto the surface of SiO_2 nanospheres successfully, the photoluminescence spectra of SiO_2/GQDs at different excitation wavelengths and photograph under UV light are shown in Fig. S2.

3.3. ECL behavior

Furthermore, ECL behaviors of the obtained GQDs were studied in 0.1 M, pH 7.4 PBS with 5 mM H_2O_2 as coreactant. As shown in Fig. 4C, when the potential was cycled negatively between −0.2 and 0.8 V, GQDs showed an intense ECL emission at 0.8 V, with an onset potential at about 0.4 V (curve a). No obvious ECL was observed in the absence of H_2O_2 (curve c), indicating the important role of H_2O_2 as coreactant. To obtain the optimum concentration of H_2O_2, The effect of concentration of H_2O_2 on the ECL behavior of GQDs was investigated. The experimental results showed that the ECL intensity increases with increasing concentration of H_2O_2, and tends to steady value after 5 mM (shown in Fig. S3 in supplemental information). Therefore, the optimal concentration of H_2O_2 is 5 mM. Meanwhile, the ECL behaviors of graphene and GO were also investigated (not shown). The results indicated that, in comparison with GQDs, the same concentration of graphene and GO had no obvious ECL signal. An attractive merit of GQDs in ECL study is the well-defined ECL peak at relatively low potential in comparison with previously reported GQDs, carbon and silicon nanocrystals (NCs) (Ding et al., 2002; Zheng et al., 2009; Dong et al., 2010; Bae et al., 2006). This merit might also profit from the newly synthetic method leading to high content of sp^2 carbon domains in GQDs inherited from graphene, which could accelerate electron transport during ECL process. ECL measurements of the GQDs upon continuous cyclic scans in PBS showed constant signals with relative standard deviation (RSD) of 1.0% (Fig. 4D), indicating the excellent stability.

To investigate the possible ECL mechanism in this system, a series of experiments were conducted. In pH 7.4 PBS containing H_2O_2, in the absence of GQDs, no ECL emission was observed (not shown). Evidently, the ECL behavior of GQDs is similar to that of other semiconductor nanocrystals, such as CdSe, carbon NCs, and Si NCs (Dong et al., 2006; Bae et al., 2006). Consequently, the ECL mechanism of the GQDs was suggested to involve the formation of excited-state GQDs (GQDs*) through electron-transfer (ET) annihilation of negatively and positively radical species.

Consequently, the ECL mechanism of the GQDs was proposed as follows: The electrooxidation of GQDs can produce the cation radicals $GQDs^{\bullet+}$ radicals, which showed an electrooxidation peak at 0.4 V (Fig. 4C, curve b). HOO^- was oxidized to O_2^-, while HOO^- was produced from the ionization balance of H_2O_2 in solution (Cui et al., 2003, 2004; Dong et al., 2006). Then, the formed O_2^- radicals and $GQDs^+$ can lead to the formation of excited-state GQDs* (Wang et al., 2009), and finally emitted light. Based on these experimental results and previous reports, the possible ECL process was described as the following equations:

$$GQDs - e^- \rightarrow GQDs^{\bullet+} \quad (1)$$

$$H_2O_2 \rightleftharpoons H^+ + HOO^- \quad (2)$$

$$HOO^- - e^{\bullet-} \rightarrow HOO^{\bullet} \leftrightarrow O_2^{\bullet-} \quad (3)$$

$$GQDs^{\bullet+} + O_2^{\bullet-} \rightarrow GQDs^* \quad (4)$$

$$GQDs^* \rightarrow GQDs + hv \quad (5)$$

3.4. The analytical performance of ECL aptamer sensor

On the basis of their intense ECL, GQDs were applied in the determination of ATP. To further improve its applicability in analytical chemistry, coating GQDs on SiO_2 nanospheres surface to make novel labels (SiO_2/GQDs) was carried out. In this system, ssDNA2 functionalized with signal amplification composites (SiO_2/GQDs) as

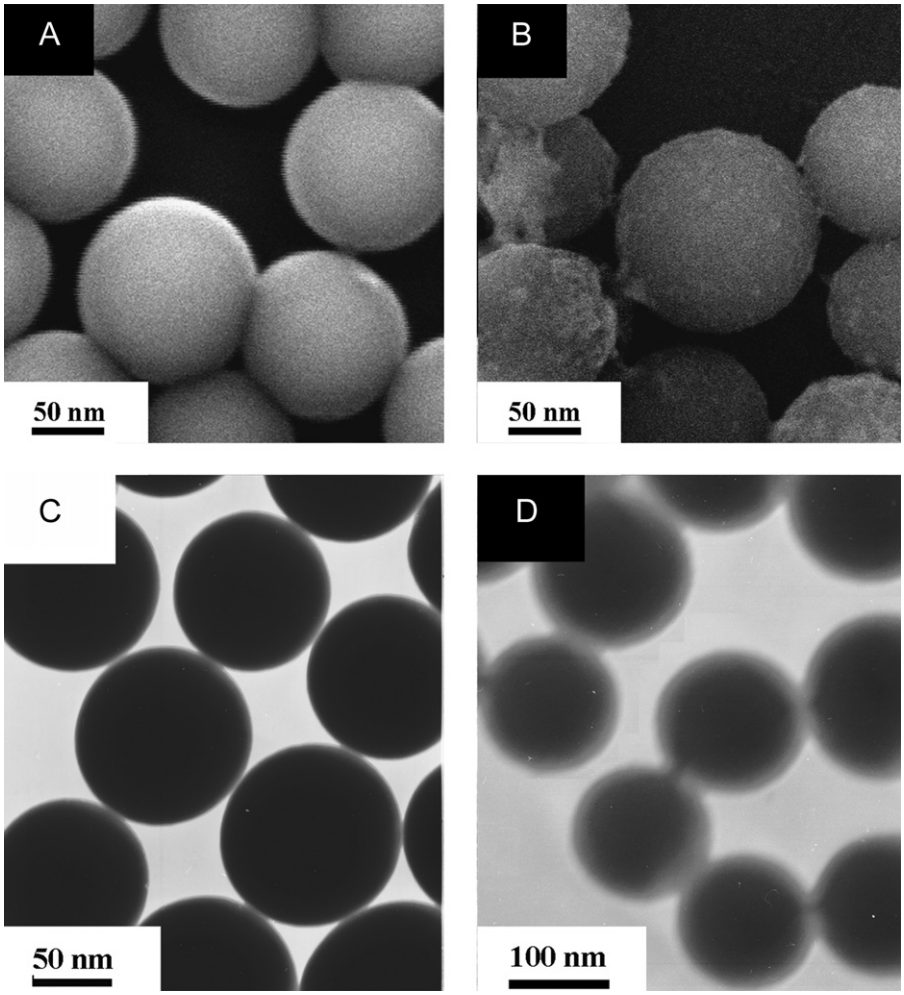

Fig. 3. Representative SEM images of SiO_2 nanospheres (A) and SiO_2/GQDs (B), TEM images of SiO_2 nanospheres (C) and SiO_2/GQDs (D).

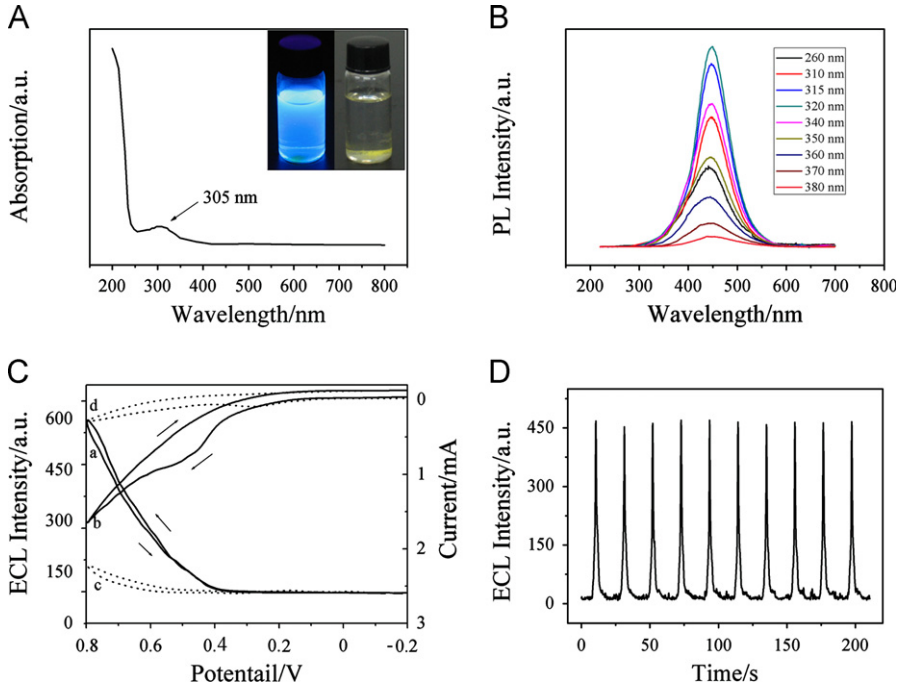

Fig. 4. The optical properties of the GQDs. (A) UV–vis absorption spectra of the GQDs aqueous solution (inset: photograph taken under UV light). (B) Photoluminescence spectra of the GQDs aqueous solution at different excitation wavelengths. (C) ECL-potential curves and CV of the GQDs in 0.1 M, pH 7.4 PBS in the presence (solid line) and absence (dotted line) of 5 mM H_2O_2. (D) ECL responses of GQDs–H_2O_2 system during a continuous potential scan between −0.2 and 0.8 V.

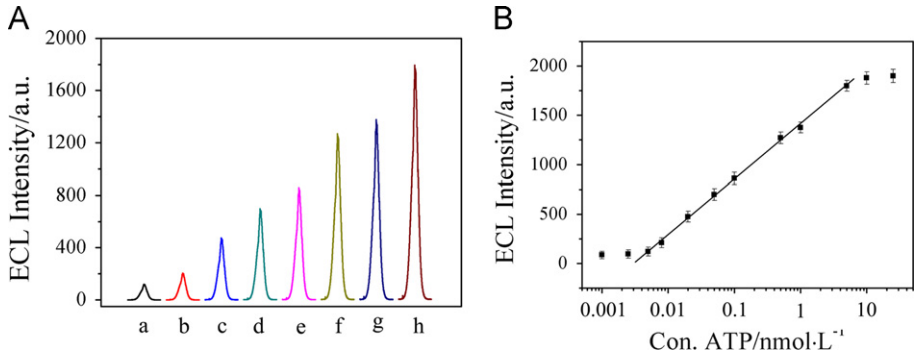

Fig. 5. (A) ECL intensity curves at different ATP concentrations. (a) 5.0×10^{-12}; (b) 8.0×10^{-12}; (c) 2.0×10^{-11}; (d) 5.0×10^{-11}; (e) 1.0×10^{-10}; (f) 5.0×10^{-10}; (g) 1.0×10^{-9}; (h) 5.0×10^{-9} mol L^{-1}. (B) The relationship between the ECL intensity (average of three times detection) and the ATP concentration.

Table 1
Comparison of the present ECL aptamer sensor with other reported sensors.

Detection method	Concentration range (mol L^{-1})	Detection limit (mol L^{-1})	Refs.
Colorimetry	4.4×10^{-6}–1.327×10^{-4}	6×10^{-7}	Wang et al. (2007)
Chemiluminescence	3.9×10^{-7}–9.96×10^{-5}	1.38×10^{-7}	Ruiz et al. (2003)
Fluorometric method	4.0×10^{-5}–5.0×10^{-6}	1.0×10^{-7}	Kanekiyo et al. (2004)
Electrochemical method	1.0×10^{-6}–4.0×10^{-3}	1.0×10^{-6}	Zuo et al. (2009)
Electrochemiluminescence	5.0×10^{-12}–5.0×10^{-9}	1.5×10^{-12}	Present work

detection probe, which provide a promising platform for the development of high-performance ECL aptamer sensor.

In the presence of ATP, owing to the formation of a stable complex between the ssDNA1 and SiO_2/GQDs modified ssDNA2, SiO_2/GQDs are caused to be immobilized onto the electrode surface, which resulting in ECL signal. However, in the absence of ATP, there is inferior interaction between the two fragments, which results in a weak ECL signal from the electrode (the corresponding data graph is shown in Fig. S4). The effect of incubation time and detection solution pH on the ECL signals of the ECL aptamer sensor is displayed in Fig. S5 (details in supporting information).

As shown in Fig. 5, under the optimized experimental conditions, the change of ECL intensity depends on the concentrations of ATP. The measurement is performed in PBS (pH = 7.4) containing H_2O_2 (5 mM), and the concentration of ATP in the testing buffer is varied from 5.0×10^{-12} mol L^{-1} to 5.0×10^{-9} mol L^{-1}. The linear regression equation was calculated as ΔI/a.u. = 560 log[ATP]+6448 (R = 0.9981) with a detection limit (LOD) of 1.5×10^{-12} mol L^{-1} at a signal-to-noise ratio of 3σ (where σ is the standard deviation of the blank solution, n = 11). The limit of quantitation (LOQ) is 5×10^{-12} mol L^{-1}. Compared with other methods reported previously (Wang et al., 2007; Ruiz et al., 2003; Kanekiyo et al., 2004; Zuo et al., 2009), our proposed ECL aptamer sensor exhibited a satisfactory detection limit, and the characteristics of other ATP sensors are summarized in Table 1.

3.5. Selectivity, reproducibility, stability of the ECL aptamer sensor

Under the optimized experimental conditions, the three ATP analogs of CTP, GTP and UTP (all concentrations are 5.0×10^{-10} mol L^{-1}) are employed to examine the selectivity of the sensor to ATP (1×10^{-11} mol L^{-1}). As illustrated in Fig. S6 (see in supporting information), the enhanced ECL intensities from the analogs are very low, but it increases greatly from ATP. The comparative results show that the proposed ECL aptamer sensor has an excellent selectivity to ATP.

The reproducibility of the aptamer sensor was examined. Sensing interfaces prepared on the same and on different electrodes were used to detect ATP with the same concentration. Standard deviation of five dependent measurements was less than 4% for the same electrode, and less than 6% for different electrodes. Thus, the aptamer sensor has a relatively good reproduction in detection.

Stability of this aptamer sensor is a key factor in their application and development. When the ECL aptamer sensor was dried and stored at 4 °C, it retained at 90% of its initial response after a storage period of 30 days, indicating the proposed ECL aptamer sensor had stable storage stability.

4. Conclusions

In summary, a novel anodic ECL was observed from GQDs for the first time by using H_2O_2 as coreactant. The ECL mechanism and photoluminescence properties were also studied. By combining intense ECL of GQDs and aptamer technique, a novel ECL aptamer sensor was proposed for measuring ATP. Furthermore, as an amplified element, SiO_2/GQDs composites were used to produce an amplified ECL signal and improve the sensitivity of the sensor. The proposed ECL aptamer sensor showed high sensitivity, good precision, acceptable stability, reproducibility, and with the detection limit of 1.5×10^{-12} mol L^{-1}. Moreover, due to the low cytotoxicity and excellent biocompatibility, GQDs are demonstrated to be an eco-friendly material as well as excellent ECL labeling agents.

Acknowledgments

This work was financially supported by Natural Science Research Foundation of China (21277058, 21175058, 21207048), Natural Science Foundation of Shandong Province, China (ZR2012BZ002) and Technology Development Plan of Shandong Province, China (Grant no. 2011GGB01153).

Appendix A. Supporting information

Supplementary data associated with this article can be found in the online version at http://dx.doi.org/10.1016/j.bios.2013.03.039.

References

Bae, Y., Lee, D.C., Rhogojina, E.V., Jurbergs, D.C., Korgel, B.A., Bard, A.J., 2006. Nanotechnology 17, 3791–3797.
Bae, Y., Myung, N., Bard, A.J., 2004. Nano Letters 4, 1153–1161.
Chen, L.Y., Chen, C.L., Li, R.N., Li, Y., Liu, S.Q., 2009. Chemical Communications 19, 2670–2672.
Cui, H., Xu, Y., Zhang, Z.F., 2004. Analytical Chemistry 76, 4002–4010.
Cui, H., Zou, G.Z., Lin, X.Q., 2003. Analytical Chemistry 75, 324–331.
Derfus, A.M., Chan, W.C., Bhatia, S.N., 2004. Nano Letters 4, 11–18.
Ding, Z., Quinn, B.M., Haram, S.K., Pell, L.E., Korgel, B.A., Bard, A.J., 2002. Science 296, 1293–1297.
Dong, Y.P., Cui, H., Wang, C.M., 2006. Journal of Physical Chemistry B 110, 18408–18414.
Dong, Y.Q., Zhou, N.N., Lin, X.M., Lin, J.P., Chi, Y.W., Chen, G.N., 2010. Chemistry of Materials 22, 5895–5899.
Eda, G., Lin, Y.Y., Mattevi, C., Yamaguchi, H., Chen, H.A., Chen, I.S., 2010. Advanced Materials 22, 505–509.
Ellington, A.D., Szostak, J.W., 1990. Nature 346, 818–822.
Famulok, M., Hartig, J.S., Mayer, G., 2007. Chemical Reviews 107, 3715–3743.
Fang, L.Y., Lu, Z.Z., Wei, H., Wang, E.K., 2008. Analytica Chimica Acta 628, 80–86.
Hu, L.D., Xu, G.B., 2010. Chemical Society Reviews 39, 3275–3304.
Jie, G., Li, L., Chen, C., Xuan, J., Zhu, J.J., 2009. Biosensors and Bioelectronics 24, 3352–3358.
Joo, J.B., Zhang, Q., Lee, I., Dahl, M., Zaera, F., Yin, Y.D., 2012. Advanced Functional Materials 22, 166–174.
Jose, D.A., Mishra, S., Ghosh, A., Shrivastav, A., Mishra, S.K., Das, A., 2007. Org. Lett. 9, 1979–1982.
Kanekiyo, Y., Naganawa, R., Tao, H., 2004. Chemical Communications, 1006–1007.
Kosynkin, D.V., Higginbotham, A.L., Sinitskii, A., Lomeda, J.R., Dimiev, A., Price, B.K., Tour, J.M., 2009. Nature 458, 872–876.
Loh, K.P., Bao, Q., Eda, G., Chhowalla, M., 2010. Nature Chemistry 2, 1015–1024.
Li, H.T., He, X.D., Liu, Y., Huang, H., Lian, S.Y., Lee, S.T., 2011. Carbon 49, 605–609.
Li, L.L., Jing, J., Fei, R., Wang, C.Z., Lu, Q., Zhang, J.R., 2012. Advanced Functional Materials 22, 2971–2979.
Li, Y., Qi, H.L., Peng, Y.G., Gao, Q., Zhang, C.X., 2008. Electrochemistry Communications 10, 1322–1325.
Marcano, D.C., Kosynkin, D.V., Berlin, J.M., Sinitskii, A., Sun, Z.Z., Slesarev, A., 2010. ACS Nano 4, 4806–4814.
Miao, W.J., 2008. Chemical Reviews 108, 2506–2553.
Myung, N., Bae, Y., Bard, A.J., 2003. Nano Letters 3, 1053–1055.
Myung, N., Ding, Z., Bard, A.J., 2002. Nano Letters 2, 1315–1319.
Pan, D.Y., Zhang, J.C., Li, Z., Wu, M.H., 2010. Advanced Materials 22, 734–738.
Ponomarenko, L.A., Schedin, F., Katsnelson, M.I., Yang, R., Hill, E.W., Novoselov, K.S., Geim, A.K., 2008. Science 320, 356–358.
Qian, J., Zhang, C., Cao, X., Liu, S., 2010. Analytical Chemistry 82, 6422–6429.
Robert, S., Randy, S., Dana, S., 2002. Analytical Chemistry 74, 2274–2278.
Ruiz, T.P., Lozano, C., Tomas, M., Martin J, V., 2003. Analytical and Bioanalytical Chemistry 377, 189–194.
Rümmeli, M.H., Rocha, C.G., Ortmann, F., Ibrahim, I., Sevincli, H., Börrnert, F., 2011. Advanced Materials 23, 4471–4490.
Shan, Y., Xu, J.J., Chen, H.Y., 2010. Chemical Communications 46, 4187–4189.
Tuerk, C., Gold, L., 1990. Science 249, 505–510.
Wang, B.J., Wang, L., Liu, X., Liang, Z., Song, S., Li, W., Li, G., Fan, C., 2007. Advanced Materials 19, 3943–3946.
Wang, Y., Lu, J., Tang, L.H., Chang, H.X., Li, J.H., 2009. Analytical Chemistry 81, 9710–9715.
Willner, I., Zayats, M., 2007. Angewandte Chemie International Edition 46, 6408–6418.
Wu, Y., Chen, C., Liu, S., 2009. Analytical Chemistry 81, 1600–1607.
Xiao, Y., Piorek, B.D., Plaxco, K.W., Heeger, A.J., 2005. Journal of the American Chemical Society 127, 17990–17991.
Yan, X., Cui, X., Li, L.S., 2010a. Journal of the American Chemical Society 132, 5944–5945.
Yang, W., Ratinac, K.R., Ringer, S.P., Thordarson, P., Gooding, J.J., Braet, F., 2010. Angewandte Chemie International Edition 49, 2114–2138.
Yuan, L., Hua, X., Wu, Y., Pan, X., Liu, S., 2011. Analytical Chemistry 83, 6800–6809.
Zheng, L.Y., Chi, Y.W., Dong, Y.Q., Lin, J.P., Wang, B.B., 2009. Journal of the American Chemical Society 131, 4564–4565.
Zhu, S., Zhang, J., Qiao, C., Tang, S., Li, Y., Yuan, W., 2011. Chemical Communications 47, 6858–6860.
Zong, J., Zhu, Y.H., Yang, X.L., Shen, J.H., Li, C.Z., 2011. Chemical Communications 47, 764–766.
Zou, G.Z., Liang, G.D., Zhang, X.L., 2011. Chemical Communications 47, 10115–10117.
Zuo, X.L., Song, S.P., Zhang, J., Pan, D., Wang, L.H., Fan, C.H., 2007. Journal of the American Chemical Society 129, 1042–1043.
Zuo, X.L., Xiao, Y., Plaxco, K.W., 2009. Journal of the American Chemical Society 131, 6944–6945.